Applied Physics A (2024) 130:86
https://doi.org/10.1007/s00339-023-07178-9

Applied Physics A
Materials Science & Processing

Check for updates

Effect of annealing temperature on solar-blind photodetectors based on 60-nm-thick Ga_2O_3 films

Shaoqing Wang[1] · Nini Cheng[1] · Guoen Zhong[1] · Xiangtai Liu[1] · Zhan Wang[1] · Haifeng Chen[1] · Yifan Jia[1] · Songang Peng[2]

Received: 6 September 2023 / Accepted: 20 November 2023 / Published online: 9 January 2024

Abstract
In this study, 60-nm-thick Ga_2O_3 films were deposited on *c*-plane sapphire substrates by atomic layer deposition process. The effect of annealing temperature on both Ga_2O_3 material and optical response characteristics was studied by ultraviolet–visible spectroscopy, X-ray diffraction and semiconductor parameter analyzer. When the annealing temperature exceeds 700 ℃, the Ga_2O_3 films exhibits a nanocrystalline β-phase. The Ga_2O_3 photoconductive solar-blind photodetectors annealed at different temperature were fabricated. The photo-current and responsivity first increase slowly and then decrease when the annealing temperature changes from 400 to 1000 ℃. An ultra-high photoresponsivity of 142 A/W with detectivity of 3.77×10^{15} Jones under 254 nm illumination was achieved for the Ga_2O_3 film annealed at 600 ℃ for 60 min in N_2/Air mixture atmosphere, which is at a very high level for ultraviolet photodetectors based on Ga_2O_3 thin films (< 100 nm). When the annealing temperature is 600 ℃, the material is in the transition stage from amorphous to crystalline state, which leads to a high degree of disorder, and further results in obvious band-tail absorption effect and improves the photoresponsivity. The results provide important guidance for the preparation of solar-blind ultraviolet detectors with ultra-high performance.

Keywords Ga_2O_3 thin films · Atomic layer deposition · Annealing temperature · Solar-blind photodetectors · Photoresponse performance

1 Introduction

Due to its strong anti-interference ability and high-wavelength selectivity, solar-blind DUV photodetectors have broad and important application prospects in many fields such as secure communication, meteorological watch, missile warning, ultraviolet astronomy, flame detection and deep space detection [1–3]. Solar-blind DUV photodetectors based on Ga_2O_3 material have attracted more and more attention because of its suitable bandgap (4.5–4.9 eV) [4], low-cost, excellent chemical stability [5] and strong irradiation hardness [6–8]. At present, there are many methods for the growth of Ga_2O_3 films, such as mist-chemical vapor deposition (Mist-CVD) [9], halide vapor phase epitaxy (HVPE) [10], atomic layer deposition (ALD) [11], pulse laser deposition (PLD) [12] and so on [13]. Among these growth methods, the ALD process provides excellent thickness control and excellent conformal coverage on substrates. No matter what kind of growth method, the post-annealing process plays an important role in the study of Ga_2O_3 film, affecting the crystallization quality, transmissivity, surface topography and chemical composition [9, 14, 15]. In this work, 60-nm-thick Ga_2O_3 films were grown on c-plane sapphire substrates by ALD process. The effect of annealing temperature on both Ga_2O_3 material and its solar-blind photoelectric characteristics was investigated.

✉ Songang Peng
pengsongang@ime.ac.cn

[1] Xi'an University of Posts and Telecommunications, Xi'an 710121, China

[2] Institute of Microelectronics of Chinese Academy of Sciences, Beijing 10029, China

2 Experimental

In this work, the ALD (Veeco, PEALD system) was used to deposit Ga_2O_3 films on c-plane sapphire with the sample station temperature of 250℃. The sources of Ga atoms and O atoms are trimethyl gallium and ozone, respectively. The chamber pressure was approximately 0.28 Torr. Ar gas was used as the purge gas. The typical ALD sequence is shown in Fig. 1. The thicknesses of Ga_2O_3 films were 60 nm for 900 cycles, which was measured by spectroscopic ellipsometry. The deposition rate is about 0.67 Å per cycle. These Ga_2O_3 films were annealed at different temperature in the air/N_2 mixture atmosphere for 60 min.

To study the influence of annealing temperature on Ga_2O_3 material and Ga_2O_3-based photodetectors, the annealing temperature was set to 400 ℃, 500 ℃, 600 ℃, 700 ℃, 800 ℃, 900 ℃ and 1000 ℃, respectively. A UV–Vis spectroscopy was used to obtain the transmittance spectra. The GIXRD spectra of as-grown and annealed Ga_2O_3 films were measured, with a grazing angle of 0.5°. The chemical element composition of these Ga_2O_3 films was analyzed by X-ray photoelectron spectroscopy spectrometer using a monochromatic Al Kα (1468.68 eV, 160 W) X-ray source.

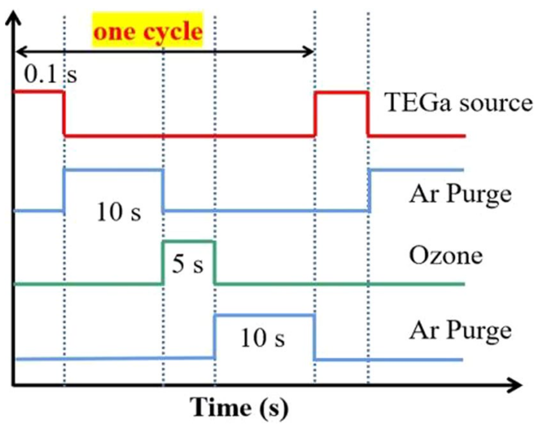

Fig. 1 The process flow of ALD Ga_2O_3 films

High-resolution scan analyses were performed to obtain the spectra of C 1s, O 2s, Ga 3d, Al 2p with a pass energy of 20 eV.

The metal–semiconductor–metal (MSM) solar-blind photodetectors were fabricated based on the prepared Ga_2O_3 films. The current–voltage and time-dependent characteristics of these photodetectors were tested using a Keysight B1505A analyzer. The photocurrents were obtained when the 254 nm light is on with an intensity of 1000 μW/cm^2. The wavelength-dependent photoresponse was conducted by a spectral measurement system (DSR-Micros-X150A-ZKDDZ).

3 Results and discussions

3.1 Characterization of Ga_2O_3 films with different annealing temperature grown on sapphire substrates

Figure 2a shows the GIXRD patterns of Ga_2O_3 films annealed at 500 ℃, 600 ℃, 700 ℃, 900 ℃ and 1000 ℃. There is no clear diffraction peak for the Ga_2O_3 film annealed at 500 ℃ and 600 ℃. While the samples show two obvious peaks in each XRD pattern after annealing at 700 ℃, 900 ℃, and 1000 ℃, respectively. The peaks located at 18.9° and 31.8° are corresponding to (-201) and (-202) of β-Ga_2O_3 (JCPDS no. 41-1103), respectively [16]. The diffraction peaks are small and broad, corresponding to the nanocrystalline nature of the 60 nm-thick Ga_2O_3 films [17]. It is worth noting that the position of (-201) and (-202) of β-Ga_2O_3 thin film for the sample annealed at 1000℃ shifts slightly to higher 2θ value, as shown in Fig. 2b. To determine the

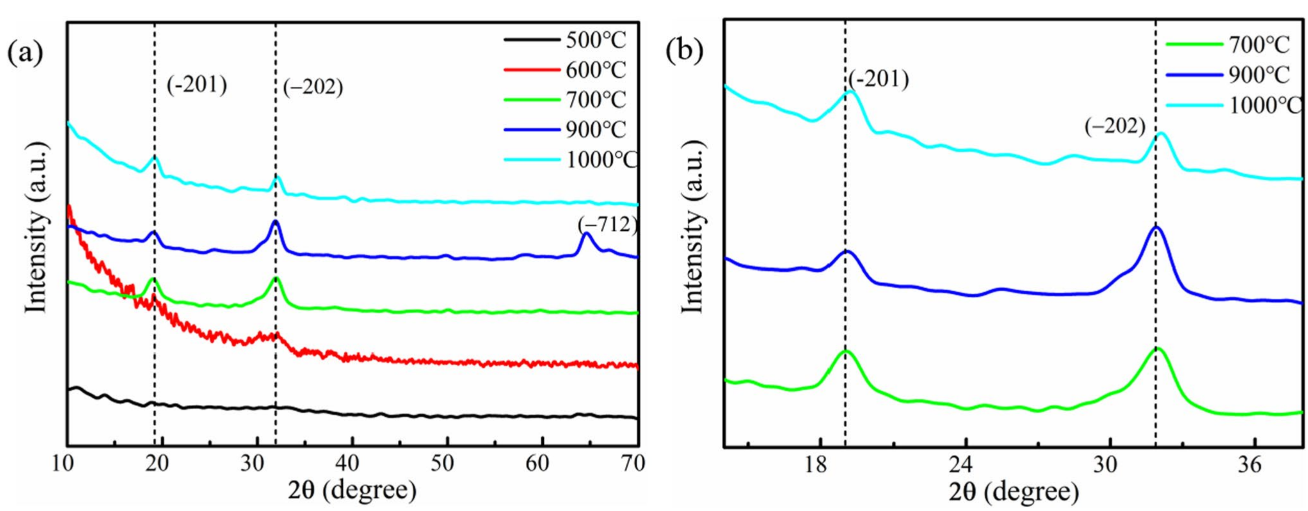

Fig. 2 **a** GIXRD patterns of Ga_2O_3 films with different annealing for 60 min, and **b** the enlarged image of XRD patterns for Ga_2O_3 films annealed at 700 ℃, 900 ℃ and 1000 ℃, respectively

reason of peak shift for the Ga_2O_3 film annealed at 1000 ℃, the XPS spectra of as-deposited and annealed at 1000 ℃ Ga_2O_3 films were measured. Figure 3 presents the XPS fine spectrum of Al 2p for Ga_2O_3 films as-deposited and annealed at 1000 ℃. There is no Al 2p peak for the as-deposited Ga_2O_3 film, while it is obvious for the sample annealed at 1000 ℃. XPS is a typical surface analysis method, which provides information about the content and morphology of elements on the surface of a sample, rather than the composition of the sample as a whole. The information depth is about 3–5 nm. Therefore, the results clearly show that the Al diffuses into the surface of Ga_2O_3 thin film from the sapphire substrate after higher temperature annealing [18]. The atomic percent of Al, Ga and O atoms for Ga_2O_3 film annealed at 1000 ℃ were 11.95%, 35.53% and 52.52%, which were determined by integrating the peak areas of Al, Ga and O. Therefore, the Al/(Al + Ga) ratios of the Ga_2O_3 films annealed at 1000℃ are about 0.25. Thus, we conclude that the position shift of (-201) and (-202) of β-Ga_2O_3 thin film for the sample annealed at 1000 ℃ is mainly caused by the Al diffusion into Ga_2O_3 films. Because the atomic radius of Al is smaller than that of Ga, the corresponding interplanar spacing (*d*-spacing) decreases. To satisfy the Bragg formula of $2d\sin\theta = n\lambda$, the Bragg angle θ increases slightly [19].

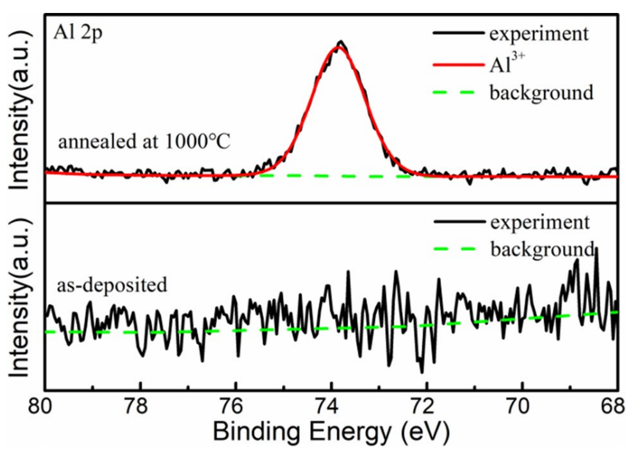

Fig. 3 The Al 2p fine spectrum of Ga_2O_3 films as-deposited and annealed at 1000 ℃

The transmittance spectra of Ga_2O_3 films annealed at different temperature are shown in Fig. 4. The average transmittance of all the samples is above 85% in visible band. The samples annealed at 800 ℃, 900 ℃ and 1000 ℃ have more transparency in the solar-blind waveband (200–280 nm) than other samples annealed at low temperature. For the direct band-gap semiconductor materials, the absorption coefficient α and bandgap E_g satisfies the following expression [20, 21]:

$$\alpha\beta\upsilon \propto (h\upsilon - E_g)^{1/2}, \tag{1}$$

where $h\upsilon$ is photon energy. The bandgap can be estimated by extrapolating the linear section of the plot $((ah\upsilon)^2 \sim h\upsilon)$ to energy axis. Figure 4b shows the relationship of $(ah\upsilon)^2$ on photon energy $h\upsilon$ for Ga_2O_3 films with different annealing temperature. The optical bandgaps of Ga_2O_3 films as-deposited and annealed at low temperature (400–700 ℃) are between 4.8 and 5.0 eV. When the annealing temperature of Ga_2O_3 films exceeds 800 ℃, the optical bandgap

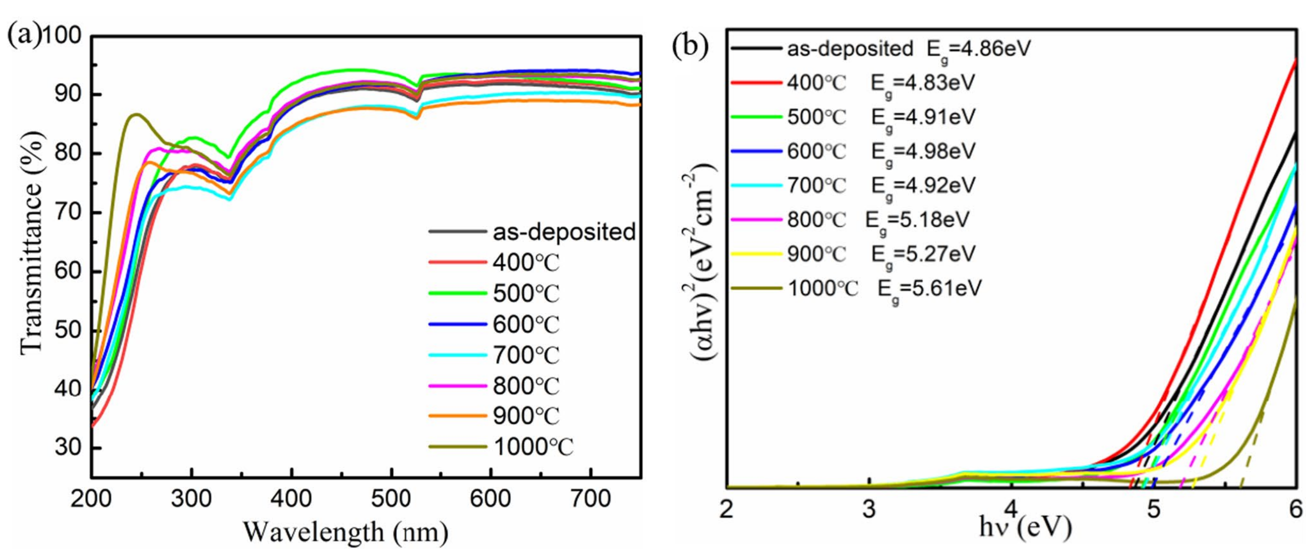

Fig. 4 **a** The transmittance spectra of all samples in the waveband of 200–800 nm. **b** $(ah\nu)^2$ versus $h\nu$ spectrum for Ga_2O_3 films on sapphire substrate

increases obviously. The optical bandgaps of the three sample annealed at 800 ℃, 900 ℃ and 1000 ℃ are 5.18 eV, 5.27 eV and 5.61 eV, respectively. β-Ga_2O_3 is a ultra-wide band-gap material with direct bandgap of ~ 4.9 eV at room temperature, while the bandgap of the isostructural θ-Al_2O_3 (monoclinic crystal system) is about 7.24 eV, greater than the bandgap of Ga_2O_3 [22]. The bandgaps becomes larger as the annealing temperature increases. There are two main reasons for the increase of optical bandgap. On one hand, the defects are suppressed as the annealing temperature increases [23], which improves the crystalline quality [24]. On the other hand, for the sample annealed at 1000 ℃, the Al diffuses into the Ga_2O_3 film from the substrate, forming $(Al_xGa_{1-x})_2O_3$ alloy [22].

3.2 Photoelectric characteristic analysis of Ga_2O_3 films with different annealing temperature

To study the effect of annealing temperature on optoelectrical properties of Ga_2O_3 thin films, interdigital photodetectors were fabricated based on them. 5 pairs of interdigitated electrodes with 300 μm in length, 50 μm in width and 10 μm in space were evaporated by e-beam evaporation equipment, following the traditional lift-off techniques. The *I–V* curves in the dark and 254 nm UV illumination are shown in Fig. 5. When the light is on, if the energy of the photon is equal to or greater than the band-gap width of the semiconductor, the electrons in the valence band will absorb the photon energy and then transition to the conduction band, producing an electron–hole pair. Thus, the free carrier concentration increases rapidly and the conductivity increases significantly. The applied voltage sweeps from − 20 to 20 V in steps of 200 mV. The MSM PDs of as-deposited and annealed at 400 ℃, 500 ℃, 600 ℃, 700 ℃, 800 ℃, 900 ℃ and 1000 ℃ Ga_2O_3 films annealed were designated as S1, S2, S3, S4, S5, S6, S7 and S8, respectively.

Compared with the other samples, both the dark current and photo-current of S4 are the largest. At the bias of 10 V, the dark currents of all samples except S4 is on the order of 10^{-13} A. The photo-current varies between 10^{-12} and 10^{-4} A for different samples at the bias of 10 V. Therefore, the effect of annealing temperature on the photoelectric properties of Ga_2O_3 MSM PDs is very significant. To further compare the performance of these photodetectors, the photo-to-dark current ratio (PDCR), light responsivity (*R*), detectivity (*D**) and external quantum efficiency (EQE) were calculated at the bias of 10 V. The responsivity *R* can be calculated by the following formula (2):

$$R = \frac{(I_{\text{photo}} - I_{\text{dark}})}{P \times S}, \quad (2)$$

where *P* and *S* are the irradiation intensity at the surface of the photodetector and effective radiation area of the photodetectors, respectively [25]. The specific detectivity (*D**) is calculated by Eq. (3)

$$D* = \frac{R}{\sqrt{2qI_{\text{dark}}/S}}, \quad (3)$$

where *q* is the electron charge [26]. The *EQE* is obtained by Eq. (4)

$$\text{EQE} = \frac{h\upsilon R}{q}, \quad (4)$$

where $h\upsilon$ is referred to the photo's energy [25]. All of the photo-current, dark current, *R*, EQE, I_{photo}/I_{dark} and *D** of Ga_2O_3 MSM PDs are listed in Table 1.

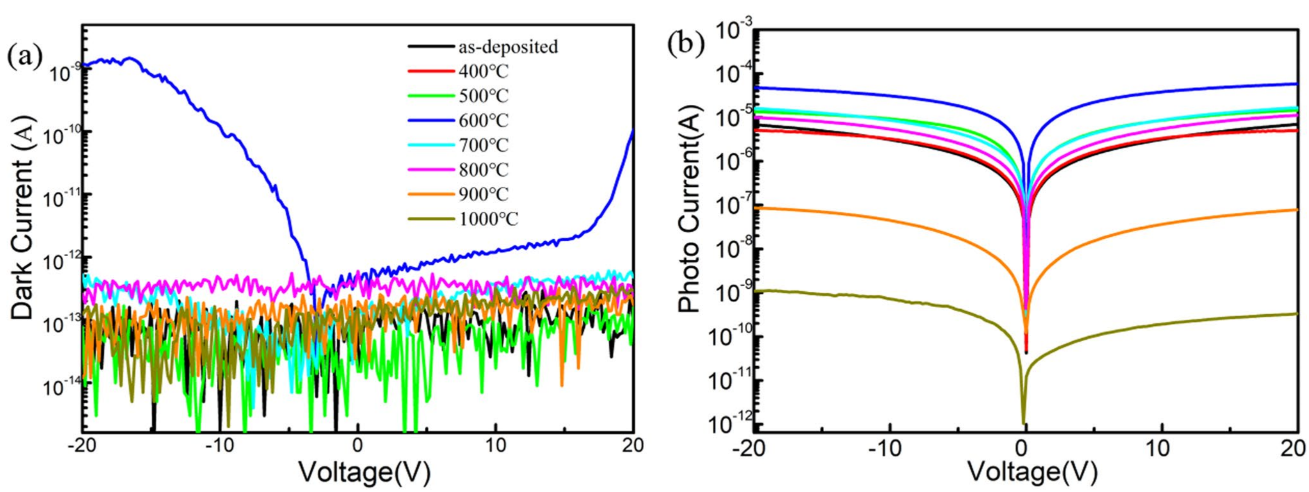

Fig. 5 The *I–V* curves of these photodetectors based on Ga_2O_3 films with different temperature annealing **a** in dark and **b** with 254 nm UV light

Table 1 The key parameters of PDs annealed at different temperature

Annealing temperature	I_{photo} (A)	I_{dark} (A)	I_{photo}/I_{dark}	Responsivity (A/W)	EQE (%)	Detectivity (Jones)	Decay time (ms)
As-deposited	3.17×10^{-6}	2.15×10^{-13}	1.47×10^{7}	11.74	5.7×10^{3}	7.35×10^{14}	33
400 ℃	3.35×10^{-6}	3.81×10^{-13}	8.79×10^{6}	12.40	6.07×10^{3}	5.84×10^{14}	26
500 ℃	8.60×10^{-6}	7.70×10^{-14}	1.12×10^{8}	31.85	1.56×10^{4}	3.33×10^{15}	32
600 ℃	**3.82×10^{-5}**	**1.19×10^{-12}**	**3.21×10^{7}**	**141.66**	**6.93×10^{4}**	**3.77×10^{15}**	**58**
700 ℃	8.72×10^{-6}	3.81×10^{-13}	2.29×10^{7}	32.30	1.58×10^{4}	1.52×10^{15}	38
800 ℃	5.53×10^{-6}	3.81×10^{-13}	1.45×10^{7}	20.48	1.00×10^{4}	9.64×10^{14}	23
900 ℃	3.65×10^{-8}	2.46×10^{-13}	1.48×10^{5}	0.14	66.14	7.92×10^{12}	20
1000 ℃	1.93×10^{-10}	3.19×10^{-13}	6.07×10^{2}	7.15×10^{-4}	0.35	3.68×10^{10}	33

The dependence of photoelectric parameters on annealing temperature of Ga_2O_3 films under 254 nm DUV illumination can be obtained from Table 1. The Ga_2O_3 films grown by ALD process in our experiment generally have ultra-low dark currents (10^{-14}–10^{-12} A). The photo-current and responsivity have the same variation trend as the annealing temperature increases. The I_{photo} and R increase first and then decrease. Once the annealing temperature of Ga_2O_3 films exceeds 800 ℃, the photoelectric performance drops sharply. Combined with XPS and transmission spectrum analysis, we can deduce that the forming of $Al_xGa_{1-x}O$ material greatly weakens the device's response to 254 nm wavelength, because of the large optical bandgap. The highest values of all the above parameters except PDCR are corresponding to the sample S4, which is annealed at 600 ℃ for 60 min before the device preparation. The R, EQE and D^* of S4 at bias of 10 V are 141.66 A/W, 69, 288% and 3.77×10^{15} Jones, respectively. From the XRD pattern shown in Fig. 2a, when the annealing temperature is 600 ℃, the material is in the transition stage from amorphous to crystalline state. Therefore, the Sample 4 has a high degree of disorder, which results in obvious band-tail absorption effect and improved the photo responsivity. The responsivity, EQE and specific detectivity are at a very high level for UV photodetectors based on Ga_2O_3 thin films (< 100 nm).

The wavelength dependence related with the responsivity for our MSM PDs with different annealing temperature at 10 V bias was also measured at room temperature, as presented in Fig. 6. The photo-response spectrum cannot be obtained because of the extremely small photo-current for sample annealed at 1000 ℃. All devices exhibit considerable sensitivities in the solar-blind band. For the as-deposited and 400 ℃ annealed samples, they have almost identical response (almost coincidence of curves), which indicates annealing temperature below 400° has little effect on material properties. For the samples annealed at 500 ℃ and 600 ℃, the photo-response is quite strong. However, once the annealing temperature is above 700 ℃, the responsivity drops rapidly. Notably, there is a slight blue shift in the peak wavelength for the samples annealed at 800 ℃ and 900 ℃. On the one hand, the annealing temperature affects crystal structure [18, 23], defect concentration [27, 28] and material composition [22]. On the other hand, the shifts of peak wavelength could be caused by the Al diffusion into the Ga_2O_3 thin film from the sapphire substrate. Both of them will cause the increase of bandgap, making the corresponding response wavelength to shift blue.

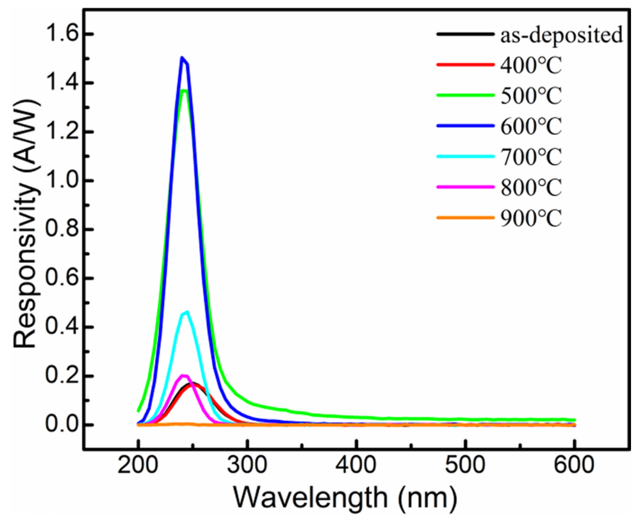

Fig. 6 The photo-response spectra of Ga_2O_3 MSM PDs

Furthermore, the time-dependent current characteristics for Sample annealed at 600 ℃ were tested using a timing switch to turn on or off the 254 nm light source. From Fig. 7a, the photo-current and dark-current show good repeatability and stability. The rise curve and decay curve can be fitted by a bi-exponential decay relaxation equation [29]

$$I = I_0 + Ae^{-(t-t_0)/\tau_1} + Be^{-(t-t_0)/\tau_2}, \quad (5)$$

where τ_1 and τ_2 represent fast and slow response time, respectively. For the rise process, the extracted rise times

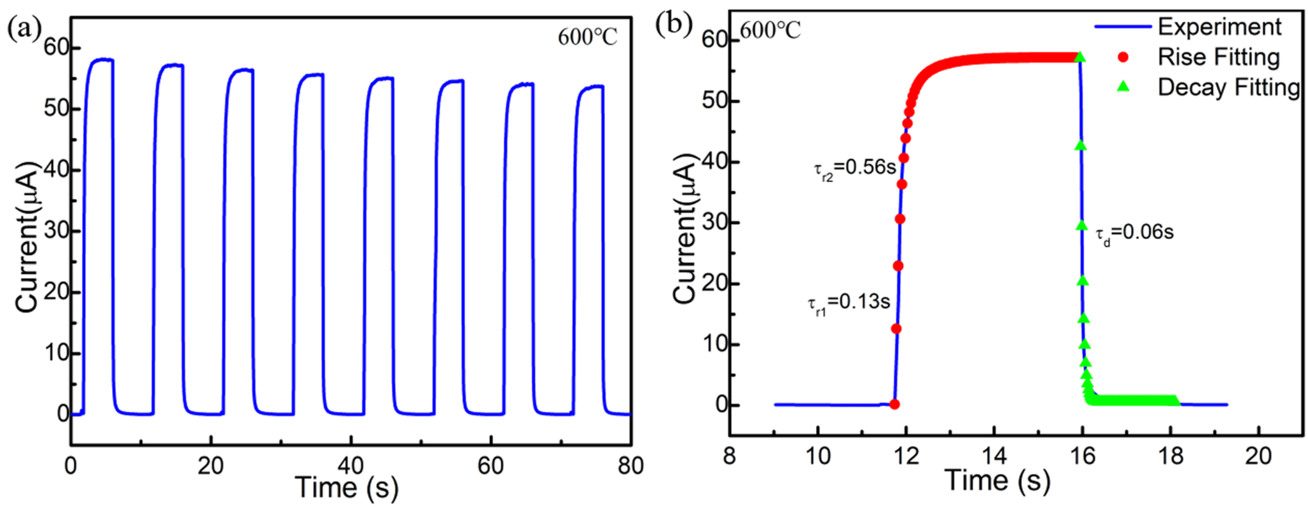

Fig. 7 **a** The time-dependent photo-response curve of Sample S4. **b** The partial enlargement of the photo-response curves and the fitting curve of the double exponential relaxation equation

τ_{r1} and τ_{r2} are 0.13 s and 0.56 s, respectively. The decay times τ_{d1} and τ_{d2} have same value of $\tau_{d1} = \tau_{d2} = 0.06$ s for the decay process. Following this fitting method, the decay time of all samples can be obtained, listed in Table 1. The decay time of PDs is mainly related to the trapping effect of the oxygen vacancy [1, 30]. The modulation of oxygen vacancy has always been the focus of Ga_2O_3 photodetectors. On the one hand, oxygen vacancy defects improve light responsivity [31, 32]. On the other hand, oxygen vacancies can cause sustained photoconductive effect, leading to the slow decay time. Therefore, there is a contradiction between light responsiveness and response time by oxygen vacancy defects [1, 12, 30, 31]. In this work, the sample S4 has the slowest decay time and the highest responsivity. Therefore, it can be inferred that the sample S4 corresponding to the Ga_2O_3 film annealed at 600 ℃ has the highest oxygen vacancy concentration.

Compared with the previously reported solar-blind photodetectors based on Ga_2O_3 thin films, our MSM PDs annealed at 600 ℃ exhibits excellent performance. The comparison of key parameters of MSM-type solar-blind PDs based on Ga_2O_3 thin film is listed in Table 2.

4 Conclusion

In this work, we investigated the influence of annealing temperature on Ga_2O_3 thin films and their DUV photodetectors. The photo-current and responsivity first increase slowly and then decrease when the annealing temperature changes from

Table 2 Comparison of key parameters of MSM-type solar-blind PDs based on Ga_2O_3 thin films

Photodetectors	Film thickness (nm)	Bias (V)	PDCR	*R* (*A/W*)	D^* (Jones)	τ_d	Dark current	References
ε-Ga_2O_3	480	5	2×10^3	146	1.2×10^{13}	5.2 s	455 nA	[33]
ε-Ga_2O_3	–	10	$>5\times10^4$	286	4.73×10^{14}	5.6 ms	5 pA	[34]
β-Ga_2O_3	400	10	1.1×10^3	2.6	1.6×10^{12}	0.26	7.63 nA	[35]
Polycrystalline Ga_2O_3	200	20	>520	0.06	–	0.16 s	<0.1 nA	[36]
β-Ga_2O_3	600	20	1.1×10^5	22,000	1.1×10^{16}	0.21 s		[37]
β-Ga_2O_3 nanocrystalline	60	–	–	57	6.30×10^{11}	15.2 ms	–	[17]
α-Ga_2O_3	30	10	10^4	0.76	–	–	0.5 pA	[38]
β-Ga_2O_3	400	20	1.1×10^8	371	6.6×10^{16}	1.3 μs	512 fA	[39]
ε-Ga_2O_3	900	6	5.7×10^4	84	4.2×10^{14}	100 ms	25 pA	[11]
Amorphous	950	− 40	–	5.9×10^4	1.8×10^{14}	–	–	[40]
Amorphous	60	10	3.2×10^7	141.66	3.77×10^{15}	60 ms	1.19 pA	This work

400 to 1000 ℃. The Al diffuses into the Ga_2O_3 thin film from the sapphire substrate when Ga_2O_3 film is annealed at higher temperature. The forming of $(Al_xGa_{1-x})_2O_3$ alloy increases the optical bandgap, making the optimal response wavelength blue shift and decreasing the DUV responsivity. An ultra-high photoresponsivity of 142 A/W with detectivity of 3.77×10^{15} Jones was achieved for the 60 nm-thick Ga_2O_3 film annealed at 600 ℃ for 60 min in N_2/Air mixture atmosphere, which can be attribute the band-tail absorption effect and the higher oxygen vacancy concentration. The responsivity is at a very high level in the reported literature for ultra-thin (< 100 nm) Ga_2O_3-based photodetectors. For Ga_2O_3 devices, operation in space environment may be subjected to various irradiation, such as gamma-ray and charged particle irradiation, which will induce a lot of damage or defects [41]. Therefore, the anti-irradiation ability of Ga_2O_3-based photodetector is also one of our future research directions.

Acknowledgements This work was supported by National Natural Science Foundation of China (Grant no. 62204203), Natural Science Foundation of Shaanxi Province (no. 2022JQ-684, 2023-JC-QN-0755), and the Youth Innovation Promotion Association of Chinese Academy of Sciences (2019120).

Author contributions In this article, the author's contribution are as follows: SW: methodology and writing—original draft. NC: data curation. GZ: formal analysis and investigation. XL: reviewing and editing, and resources. ZW: investigation and resources. HC: supervision. YJ: investigation and resources. SP: conceptualization and resources.

Data availability Data are included in article/supplementary material/referenced in article.

Declarations

Conflict of interest The authors declare no competing financial or non-financial interest to disclose.

References

1. C.Q. Zhou, K.W. Liu, X. Chen, J.H. Feng, J.L. Yang, Z.Z. Zhang, L. Lei, Y. Xia, D.Z. Shen, Performance improvement of amorphous Ga_2O_3 ultraviolet photodetector by annealing under oxygen atmosphere. J. Alloy. Compd. **840**, 155585 (2020)
2. J.J. Xu, W. Zheng, F. Huang, Gallium oxide solar-blind ultraviolet photodetectors: a review. J. Mater. Chem. C **7**, 8753–8770 (2019)
3. D.Y. Guo, K. Chen, S.L. Wang, F.M. Wu, A.P. Liu, C.R. Li, P.G. Li, C.K. Tan, W.H. Tang, Self-powered solar-blind photodetectors based on α/β phase junction of Ga_2O_3. Phys. Rev. Appl. **13**, 024051 (2020)
4. M. Higashiwaki, H. Murakami, Y. Kumagai, A. Kuramata, Current status of Ga_2O_3 power devices. Jpn. J. Appl. Phys.. J. Appl. Phys. **55**, 12021 (2016)
5. H. Altuntas, I. Donmez, C. Ozgit-Akgun, N. Biyikli, Electrical characteristics of β-Ga_2O_3 thin films grown by PEALD. J. Alloy. Compd. **593**, 190–195 (2014)
6. B.R. Tak, M. Garg, A. Kumar, V. Gupta, R. Singh, Gamma irradiation effect on performance of β-Ga_2O_3 metal-semiconductor-metal solar-blind photodetectors for space applications. ECS J. Solid. State. Sci. **8**, Q3149 (2019)
7. D. Akay, U. Gokmen, S.B. Ocak, Ionizing radiation influence on rubrene-based metal polymer semiconductors: direct information of intrinsic electrical properties. JOM **72**, 2391–2397 (2020)
8. D. Akay, S. Karadeniz, A.B. Selçuk, S.B. Ocak, Effect of gamma-ray irradiation on the electrical characteristics of Al/C24H12/p-Si nano-structure. Phys. Scripta **93**, 095301 (2018)
9. Y.L. Cheng, Y. Xu, Z. Li, J.Q. Zhang, D.Z. Chen, Q. Feng, S.R. Xu, H. Zhou, J.C. Zhang, Y. Hao, C.F. Zhang, Heteroepitaxial growth of α-Ga_2O_3 thin films on a-, c-and r-plane sapphire substrates by low-cost mist-CVD method. J. Alloy. Compd. **831**, 154776 (2020)
10. B.R. Tak, S. Kumar, A.K. Kapoor, D.H. Wang, X.H. Li, H.D. Sun, R. Singh, Recent advances in the growth of gallium oxide thin films employing various growth techniques—a review. J. Phy. D Appl. Phys. **54**, 453002 (2021)
11. Y. Qin, H.D. Sun, S.B. Long, G.S. Tompa, T. Salagaj, H. Dong, Q.M. He, G.Z. Jian, Q. Liu, H.B. Lv, M. Liu, High-performance metal-organic chemical vapor deposition grown ε-Ga_2O_3 solar-blind photodetector with asymmetric schottky electrodes. IEEE Electr. Dev. Lett. **40**, 1475–1478 (2019)
12. S.H. Jeong, T.K.O. Vu, E.K. Kim, Post-annealing effects on Si-doped Ga_2O_3 photodetectors grown by pulsed laser deposition. J. Alloy. Compd. **877**, 160291 (2021)
13. A.K. Saikumar, S.D. Nehate, K.B. Sundaram, Technology. RF sputtered films of Ga_2O_3. ECS J. Solid State Sci. **8**, Q3064–Q3078 (2019)
14. J. Wang, L.J. Ye, X. Wang, H. Zhang, L. Li, C.Y. Kong, W.J. Li, High transmittance β-Ga_2O_3 thin films deposited by magnetron sputtering and post-annealing for solar-blind ultraviolet photodetector. J. Alloy. Compd. **803**, 9–15 (2019)
15. M.K. Yadav, A. Mondal, S. Das, S.K. Sharma, A. Bag, Impact of annealing temperature on band-alignment of PLD grown Ga_2O_3/Si(100) heterointerface. J. Alloy. Compd. **819**, 153052 (2020)
16. X. Li, H.L. Lu, H.P. Ma, J.G. Yang, J.X. Chen, W. Huang, Q.X. Guo, J.J. Feng, D.W. Zhang, Chemical, optical, and electrical characterization of Ga_2O_3 thin films grown by plasma-enhanced atomic layer deposition. Curr. Appl. Phys.. Appl. Phys. **19**, 72–81 (2019)
17. M.I. Pintor-Monroy, B.L. Murillo-Borjas, M.A. Quevedo-Lopez, Nanocrystalline and polycrystalline β-Ga_2O_3 thin films for deep ultraviolet detectors. ACS Appl. Electron. Ma. **2**, 3358–3365 (2020)
18. A. Goyal, B.S. Yadav, O.P. Thakur, A.K. Kapoor, R. Muralidharan, Effect of annealing on β-Ga_2O_3 film grown by pulsed laser deposition technique. J. Alloy. Compd. **583**, 214–219 (2014)
19. C.H. Liao, K.H. Li, C.G. Torres-Castanedo, G.Z. Zhang, X.H. Li, Wide range tunable bandgap and composition β-phase $(AlGa)_2O_3$ thin film by thermal annealing. Appl. Phys. Lett. **118**, 032103 (2021)
20. A. Chmielewski, Z.L. Deng, M. Saleh, J. Jesenovec, W. Windl, K. Lynn, J. McCloy, N. Alem, Atomic-scale characterization of structural and electronic properties of Hf doped β-Ga_2O_3. Appl. Phys. Lett. **119**, 172102 (2021)
21. C.L. Sun, Z.P. Wu, S.J. Lu, Z. Ren, Y.H. An, D.Y. Guo, X.C. Guo, X.L. Chu, W.H. Tang, Determination of the optical constants of Gallium oxide films. Adv. Mat. Res. **986**, 42–46 (2014)
22. J.B. Varley, A. Perron, V. Lordi, D. Wickramaratne, J.L. Lyons, Prospects for n-type doping of $(Al_xGa_{1-x})_2O_3$ alloys. Appl. Phys. Lett. **116**, 172104 (2020)

23. A.K. Singh, M. Gupta, V. Sathe, Y.S. Katharria, Effect of annealing temperature on β-Ga_2O_3 thin films deposited by RF sputtering method. Superlatt. Microst. **156**, 106976 (2021)
24. W. Mi, K.L. Zhang, J.S. Zhao, Z.C. Yang, Annealing effect on the optical and electronic properties of β-Ga_2O_3/AZO multilayered films. J. Mater. Sci-Mater. El. **27**, 11390–11395 (2016)
25. J. Yu, L. Dong, B. Peng, L. Yuan, Y. Huang, L. Zhang, Y. Zhang, R. Jia, Self-powered photodetectors based on β-Ga_2O_3/4H–SiC heterojunction with ultrahigh current on/off ratio and fast response. J. Alloy. Compd. **821**, 153532 (2020)
26. X.H. Hou, H.D. Sun, S.B. Long, G.S. Tompa, T. Salagaj, Y. Qin, Z.F. Zhang, P. Tan, Ultrahigh-performance solar-blind photodetector based on α-phase-dominated Ga_2O_3 film with record low dark current of 81 fA. IEEE Electr. Dev. Lett. **40**, 1483–1486 (2019)
27. J. Jesenovec, M.H. Weber, C. Pansegrau, M.D. McCluskey, K.G. Lynn, J.S. McCloy, Gallium vacancy formation in oxygen annealed β-Ga_2O_3. J. Appl. Phys. **129**, 245701 (2021)
28. R.J. Sun, Y.K. Ooi, P. Ranga, A. Bhattacharyya, S. Krishnamoorthy, M.A. Scarpulla, Oxygen annealing induced changes in defects within β-Ga_2O_3 epitaxial films measured using photoluminescence. J. Phy. D Appl. Phys. **54**, 174004 (2021)
29. J.Y. Du, J.X.C. Ge, H. Liu, P.Y. Liu, H.Y. Hao, J.J. Dong, Z.Y. Zheng, H. Gao, Highly sensitive and ultrafast deep UV photodetector based on a β-Ga_2O_3 nanowire network grown by CVD. J. Phy. D Appl. Phys. **49**, 425105 (2016)
30. S. Li, J.Y. Yue, X.Q. Ji, C. Lu, Z.Y. Yan, P.G. Li, D.Y. Guo, Z.P. Wu, W.H. Tang, Oxygen vacancies modulating the photodetector performances in ε-Ga_2O_3 thin films. J. Mater. Chem. C **9**, 5437–5444 (2021)
31. R. Xu, X.C. Ma, Y.H. Chen, Y. Mei, L.Y. Ying, B.P. Zhang, H. Long, Effect of oxygen vacancies in heteroepitaxial β-Ga_2O_3 thin film solar blind photodetectors. Mat. Sci. Semicond. Proc. **144**, 106621 (2022)
32. X.Q. Ji, X.M. Yin, Y.Z. Yuan, S.Q. Yan, X.Q. Li, Z.J. Ding, X.Y. Zhou, J.W. Zhang, Q. Xin, A.M. Song, Amorphous Ga_2O_3 Schottky photodiodes with high-responsivity and photo-to-dark current ratio. J. Alloy. Compd. **933**, 167735 (2023)
33. X. Cao, Y.H. Xing, J. Han, J.S. Li, T. He, X.D. Zhang, J.H. Zhao, B.S. Zhang, Crystalline properties of ε-Ga_2O_3 film grown on c-sapphire by MOCVD and solar-blind ultraviolet photodetector. Mat. Sci. Semicond. Proc. **123**, 105532 (2021)
34. S.R. Zhou, H. Zhang, X. Peng, H.W. Liu, H.L. Li, Y.Q. Xiong, W.J. Li, P.A. Yang, Fully transparent and high-performance ε-Ga_2O_3 photodetector arrays for Solar-Blind imaging and deep-ultraviolet communication. Adv. Photon. Res. **3**, 2270037 (2022)
35. M.Q. Li, N. Yang, G.G. Wang, H.Y. Zhang, J.C. Han, Highly preferred orientation of Ga_2O_3 films sputtered on SiC substrates for deep UV photodetector application. Appl. Surf. Sci. **471**, 694–702 (2019)
36. H.T. Zhou, L.J. Cong, J.G. Ma, M.Z. Chen, D.Y. Song, H.B. Wang, P. Li, B.S. Li, H.Y. Xu, Y.C. Liu, High-performance high-temperature solar-blind photodetector based on polycrystalline Ga_2O_3 film. J. Alloy. Compd. **847**, 156536 (2020)
37. Y. Xu, Y.L. Cheng, Z. Li, D.Z. Chen, S.R. Xu, Q. Feng, W.D. Zhu, Y.C. Zhang, J.C. Zhang, C.F. Zhang, Ultrahigh-performance solar-blind photodetectors based on high quality heteroepitaxial single crystalline β-Ga_2O_3 film grown by vacuum-free, low-cost mist chemical vapor deposition. Adv. Mater. Technol-Us **6**, 2001296 (2021)
38. S.H. Lee, K.M. Lee, Y. Kim, Y. Moon, S.B. Kim, D. Bae, T.J. Kim, S. Kim, S.W. Lee, Sub-microsecond response time deep-ultraviolet photodetectors using α-Ga_2O_3 thin films grown via low-temperature atomic layer deposition. J. Alloy. Compd. **780**, 400–407 (2019)
39. Z.Y. Zheng, B.S. Qiao, Z.Z. Zhang, X.Q. Huang, X.H. Xie, B.H. Li et al., High detectivity of metal–semiconductor–metal Ga_2O_3 solar-blind photodetector through thickness regulated gain. IEEE. Trans. Electron. Dev. **69**, 4362–4365 (2022)
40. Y.H. Wang, H.R. Li, J. Cao, J.Y. Shen, Q.Y. Zhang, Y.T. Yang, Z.G. Dong, T.H. Zhou, Y. Zhang, W.H. Tang, Ultrahigh gain solar blind avalanche photodetector using an amorphous Ga_2O_3-based heterojunction. ACS Nano **15**, 16654–16663 (2021)
41. D. Akay, U. Gokmen, S.B. Ocak, Radiation-induced changes on poly (methyl methacrylate) (PMMA)/lead oxide (PbO) composite nanostructure. Phys. Scr. **94**, 115302 (2019)